A Fluorescent Probe Study of Micelle-like Cluster Formation in Aqueous Solutions of Hydrophobically Modified Poly(ethylene oxide)

Ahmad Yekta, Jean Duhamel, Pascale Brochard,[1] Hendra Adiwidjaja, and Mitchell A. Winnik*

Department of Chemistry and Erindale College, University of Toronto, Toronto, Ontario, Canada M5S 1A1

Received September 30, 1992; Revised Manuscript Received December 9, 1992

ABSTRACT: Fluorescent probes have been utilized to investigate the micellar nature of self-association in aqueous solutions of associative thickeners. The specific polymers are $C_{16}H_{33}$-end-capped urethane-coupled poly(ethylene oxide)s (HEUR's). Data are presented indicating the presence of micelle-like clusters with two-digit aggregation numbers. The clusters are the building blocks of an association network leading to the formation of microgels that persist even when the solutions are dilute and of low viscosity. The clusters have a microscopic viscosity far exceeding that of a typical surfactant micelle. Possible consequences of such rigid micelles on the interpretation of fluorescence quenching data are discussed and compared with that for surfactant micelles.

Introduction

Fluorescence probe techniques have played a powerful role in the elucidation of micelle structure and dynamics.[2] In this methodology, one adds a small amount of a fluorescent dye (the probe) to a micellar system and measures various features of the dye fluorescence. If some aspect of this fluorescence is affected by its micellar environment, these changes convey information about the microenvironment. Normally, three types of experiments are carried out. Polarity-sensitive[3-8] dyes convey information about the hydrophobicity of the dye environment in the micelle. Friction-sensitive[9-11] probes report on the mobility of the dye in the micelle (i.e., the "microviscosity" of the micelle). Fluorescence quenching experiments,[12] in which one adds both fluorophore (F) and quencher (Q) to the system and interprets the quenching data in terms of a Poisson distribution[12a] of F and Q among micelles, allow one to determine the mean association number, N_{agg}, of the micelles.

Recently, these techniques have been extended to systems involving water-soluble polymers. These applications include polymer–surfactant interactions and hydrophobic domain formation in polymers bearing hydrophobic side chains. Polysoaps and hydrophobically modified polyacrylamides are important examples. Key contributions have been made by the groups of Zana[2a] in France and Thomas[2c] in the U.S.

We wish to report fluorescence probe studies on a system which is conceptually similar to the polymer systems mentioned above. The system involves poly(ethylene oxide) polymers end-capped by hydrophobic substituents, here $C_{16}H_{33}O$ groups. These polymers were developed as shear-thinning rheology modifiers for water-borne coatings.[13] More specifically, our polymers are prepared by reacting poly(ethylene glycol), $M_n \approx 8200$ (narrow molecular weight distribution), with isophorone diisocyanate and a limiting amount of cetyl alcohol, to produce a polymer which is in fact a urethane-coupled poly(ethylene oxide) end-capped with hydrophobic substituents,[14] often referred to in the coatings industry as HEUR-type associative thickeners (AT's). The chemical structure of the polymer is shown below.

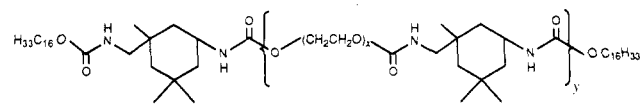

2 and **3**

$x \approx 190$

$y_2^{calc} = 4$

$y_3^{calc} = 6$

Since it is prepared by condensation coupling of a rather small number (2–10) of oligomers, the final molecular weight distribution is rather broad. There is a widespread belief that these materials promote viscosity through end-group association to form micelle-like clusters (MLC's). The polymer chains bridge the MLC's, creating a network which resists macroscopic deformation of the fluid. At high enough concentration, the network spans the solution, and the system gels.

Our previous probe experiments[15] give credence to the idea that the MLC's are indeed micelle-like. Here we provide further interesting insights into the nature of the MLC structure. The fluorescence quenching experiments, however, appear not to follow Poisson quenching kinetics. This is a completely unexpected result. Understanding this result is the major thrust of the experiments described here.

Experimental Section

Materials. The polymeric associative thickeners **2** and **3** are generous donations of Union Carbide, sample nos. 46RCHX22-2 and 46RCHX22-3, respectively.[14] In an earlier communication,[15] we had referred to these as PEO-C16/40 and PEO-C16/47, respectively. The polymers were purified by 3× dissolution (5 wt %) in warm methanol, crystallization and centrifuging at −15 °C, decanting of the cold solvent, and finally dissolution (10 wt %) and freeze-drying from benzene. The yield was 80%. These polymers were originally prepared at Union Carbide by melt condensation of a mixture of dried poly(ethylene glycol) of M_n = 8200 (narrow molecular weight distribution), isophorone diisocyanate, and *n*-hexadecyl alcohol of a well-defined stoichiometric ratio to give the desired product. Sample 46RCHX22-2 has a calculated M_n = 34 000, and sample 46RCHX22-3 has M_n = 51 000, based upon reaction stoichiometry. By gel permeation chromatography (GPC) in tetrahydrofuran (100 μL of a 0.4 wt % solution, 0.8 mL/min, through Ultrastragel columns (500 +

0024-9297/93/2226-1829$04.00/0

10^4 Å)) one observes a broad molecular weight distribution with a tail in the low-M region which includes a small peak at M = 8000 based upon poly(ethylene oxide) standards. Analysis of these traces gives $M_w \approx 52\,000$ for **2** and $M_w \approx 58\,000$ for **3**, respectively. The values obtained are very sensitive to the choice of the base line and the presence of the tail in the low-M region. Calculated polydispersity M_w/M_n values range from 1.7 to 2.2. The GPC showed little difference, within the variation described above, between the unpurified and recrystallized polymer samples. Polyethers are susceptible to oxidative degradation. Solid samples were stored at −10 °C, protected from light and humidity.

Pyrene (Aldrich) was recrystallized three times from ethanol. Dodecylpyridinium chloride monohydrate (DPCl, Aldrich) and sodium dodecyl sulfate (SDS, Aldrich) were used as received. Bis(1-pyrenyl) methyl ether ("dipyme") was the same sample as reported previously.[11] Distilled water was further purified through a Millipore Milli Q purification system.

Sample Preparation. Solutions were prepared by combining polymer with ca. 70% of the water required, stirring the solution overnight at ca. 22 °C, and then adding the exact amount (by weight) of water necessary to obtain the desired polymer concentration. Careful measurements at 20 °C of the specific gravity of the most concentrated solutions (1–2 wt %) showed them to be within 0.3% of that of pure water. Therefore, wt % units have been freely exchanged into wt/vol units. Stock solutions were kept in the dark at 10 °C and stored for not more than 2 weeks.

Pyrene Saturation Experiments. Pyrene (2.0 mg) was deposited onto the walls of several centrifuge tubes by gentle evaporation under a flow of N_2 gas of a solution (0.5 mL) of pyrene in acetone (20 mM). This quantity is 2 orders of magnitude larger that that necessary to achieve saturation of the solutions described below. To each tube was added 5.0 g of AT polymer solution of known concentration. A small magnetic stirring bar was added. The tubes were stoppered and stirred (12 h) at 22 ± 2 °C in the dark. The tubes were centrifuged (2000 rpm, 20 min) to sediment pyrene microcrystals. UV spectra were measured, and the solutions were returned to their original tubes and the stirring was continued. In this way, it was found that the less concentrated polymer solutions reached saturation levels within 2 days, while the more concentrated solutions required 4–5 days of room-temperature stirring. The difference is probably related to less efficient stirring of the more viscous solutions. The 10 g/L solutions of **2** were too viscous to saturate in this way. For excimer studies described below, a nearly saturated pyrene solution of **2** was made by adding the solution to an exact quantity of pyrene crystals, stirring for 5 days at 20 °C followed by 8 h at 50 °C, and then cooling to room temperature. Dilution and UV measurements showed that the solution contained no excess pyrene crystals.

UV Absorption Measurements. A Hewlett-Packard 8452A diode-array spectrophotometer with a 2-nm resolution was used. The polymer solutions were somewhat turbid in the UV, and an equivalent polymer solution reference was used in all measurements. For pyrene solutions, the absorbance at each wavelength was taken relative to the absorbance at 400 nm. With this small internal correction (less than 0.03 absorbance units), the results were more reproducible. The extinction coefficients ϵ for micellized pyrene were evaluated by using a standard 5.0 g/L solution of **2**. At this concentration, only 2.3% of the total pyrene is in the water phase. The error due to light absorption by aqueous pyrene is even smaller because at the peak 338-nm band of micellized pyrene the ϵ of aqueous pyrene is relatively small.[16] The ϵ values of micellized pyrene at the major peaks in the spectrum are as follows (in 10^4 M^{-1} cm^{-1} units): 338 nm, 3.58; 322 nm, 2.35; 308 nm, 0.94; 274 nm, 3.22; 264 nm, 1.92; 242 nm, 5.28. The value at 338 nm is the most reliable.

Fluorescence Emission Measurements. A SPEX Fluorolog 2 spectrometer equipped with double-grating monochromators and a red-sensitive photomultiplier (PM) and photon-counting detection was used. Resolution was set at 0.50 mm (1.0 nm) or better. The spectra were recorded simultaneously in the S & R mode in 0.50-nm steps, integrating counts for 1 s. For linearity of response, the sample (S) PM counts were always kept less than 3×10^5 counts/s, and the reference (R) PM less than 0.06 μA, dependent on the excitation settings. All solutions studied were aerated (temperature controlled at 20 ± 0.5 °C), magnetically stirred, and examined at right-angle optical geometry. With the 10 g/L solution of **2**, efficient stirring was not possible. Shear forces arising from various stirring rates or repeated cycles of heating (to 50 °C) and cooling (to 20 °C) had no observable effect on intensity or the shape of the spectra. Actual sample spectra were corrected for scatter of an equivalent blank solution. This correction ranged from 0.1 to 5% of the total integrated signal. In data analysis, excimer intensities were considered only if the blank correction in the 450–550-nm interval was less than 5% of the excimer signal. Blank-corrected spectra were obtained by converting raw S & R data to S/R (separately for sample and blank) and subtracting the blank. Values of I_1/I_3 and integrals of the two domains, 365–392.5 nm (peak of I_5) and 450–550 nm excimer range, were so determined. A crucial assumption here is that the former interval corresponds to pure monomer fluorescence intensity I_M. The validity of this assumption is seen by the constancy of I_1/I_3 as the excimer intensity changes. This value is indeed a constant to within ±0.01 and slightly dependent on the excitation wavelength λ_{ex} and the polymer concentration. For λ_{ex} = 308 nm, the values of I_1/I_3 are 1.17, 1.19, and 1.21 for [**2**] being 10, 5.0, and 2.3 g/L, respectively. The fluorescence intensity in the region 450–550 nm was ascribed to excimer emission intensity I_E. Actually, this region contains a contribution from the tail of the pure monomer fluorescence spectrum. This is a constant 6% of the I_M defined above. Therefore, our calculated values of I_E/I_M are high by 0.06, which shows up as an intercept in the plots of I_E/I_M vs [Py] but has no effect on our conclusions. An example of an actual experimental run of excimer emission is as follows: weighed quantities (1.3 g) of a 10 g/L solution of **2** (loaded to near saturation with pyrene) were placed into rectangular quartz fluorescence cells each containing a small stirring bar and tightly capped. Next, weighed quantities of **2** (10 g/L, with no pyrene) were added to each cell to dilute the pyrene concentration of each solution, while the polymer concentration remained constant. The solutions were well mixed, and measurements were repeated to ensure that no time-dependent relaxation phenomena affected our measurements. When the cell was nearly full (ca. 2 mL), some of its contents were discarded and the weighing/dilution operation continued. In this way, [Py] was varied and Beer's law plots were obtained. When the full set of data was analyzed, it was discovered that fluorescence cells with a content less than 1.2 g (all samples had at least a content of more than 1.0 g, where the top meniscus of the solution was about 2 mm above the highest path of the excitation beam) consistently showed higher (ca. 10%) values of both I_E and I_M. This could be traced to the reflective character of the sample meniscus. While this effect cancels out in the ratio I_E/I_M, it will cause some outlying points when individual luminescence yields are considered. The reproducibility and stability of I_E/I_M are as follows: for repetition of experiments within the same day, ±1% for I_E and I_M individually, and better than ±0.4% for the ratio I_E/IM. When samples are stored at room temperature in the dark, I_E/I_M is reproducible to within ±1% over 2 days and shows a gradual 10% drop over 3 weeks.

Evaluation of Individual Monomer and Excimer Yields from Steady-State Data. In the experiments described above I_E and I_M reflect not only the respective luminescence quantum yields of excimer and monomer but also the total quantity of excitation light absorbed by the system under study. Since [Py] is varied, so is the light absorbed, and this must be accounted for to evaluate the individual excitation-intensity-independent yields. If we call the yields Y_E and Y_M, respectively, then it is clear that I_E/I_M equals Y_E/Y_M, and no correction is necessary for this ratio. In the right-angle geometry of luminescence, the optical correction term is [Py] $\exp\{-1.15\epsilon_\lambda[\mathrm{Py}]\}$. Here, ϵ_λ is the molar decadic extinction coefficient of micellized pyrene at the wavelength of excitation λ. The intensities I_E and I_M would have to be divided by this correction term to obtain the corresponding yields. This correction term, an approximation, works best for low optical densities (OD). For this reason, steady-state fluorescence measurements were run with excitation in the weakest absorption band of pyrene at 308 nm for the 10 and 5.0 g/L solutions of **2** where OD was high and in the stronger absorption band of pyrene at 338 nm for the 2.3 g/L solution. In this way, the maximum OD in either case did not exceed 0.5 cm^{-1}. The

ϵ_λ values used for the correction term were derived from Beer's law plots described above. These had the values (units: 10^4 M^{-1} cm^{-1}) 0.981, 0.829, and 3.05 for the above-mentioned solutions of 2, respectively. As seen in Figure 6, the ratio Y_E/Y_M is substantially free of errors involved with the optical correction term while the individual Y_E and Y_M have amplified errors due to division by [Py], a factor varying by nearly 2 orders of magnitude. Proper data analysis (see the text below) involves plotting $Y_M°/Y_M$ vs [Py], where $Y_m°$ is the pyrene monomer fluorescence yield in the limit of infinite dilution (in pyrene). $Y_M°$ is evaluated by making a plot of relative Y_M vs [Py], extrapolating the data to the intercept of [Py] $\rightarrow$ 0.

Evaluation of Individual Monomer Yields from Fluorescence Decay Data. The single-photon-timing method was used to obtain luminescence decay data of pyrene monomer (376 nm) and excimer (520 nm). The excitation was at 338 nm. The decay profiles were fitted arbitrarily to a sum of three-exponential terms of the form

$$I(t) = \sum_{j=1}^{j=3} a_j \exp(-t/\tau_j) \qquad \sum_{j=1}^{j=3} a_j = 1 \qquad (1)$$

These functions were integrated to obtain relative luminescence yields. Taking the sum of coefficients equal to unity is equivalent to normalizing different luminescence data to a hypothetical equal-optical-density experiment. Therefore, the complicated light absorption correction necessary with steady-state data is not necessary here. We have made some attempt to analyze the $I(t)$ profiles in terms of models of excimer kinetics. These results are sufficiently complicated that they will be reported separately.

Results and Discussion

In this section we first present evidence that the $C_{16}H_{33}O$ end groups of the AT polymers associate to form micelle-like clusters. Included here are measurements from which the partition coefficient (K_v) of pyrene between the aqueous and cluster phases can be calculated. We then present a microgel network model for the polymer in water in which the clusters formed by end-group association serve as the junction points. Focusing on the clusters, we review Poisson quenching kinetics which typifies quenching processes for aqueous micelles. Data are presented for quenching reactions in solutions of the AT polymers. These data are seemingly at odds with the Poisson quenching model. A major part of this section is devoted to an examination of the factors that might be responsible for the quenching kinetics we observe.

Existence of Hydrophobic Microdomains. Polarity Probes. Many aromatic dyes provide spectral evidence about the micropolarity of the dye environment.[3-8] Pyrene and many of its derivatives provide this information both through changes in the absorption spectra and through the relative intensities of bands in the fine structure of the pyrene fluorescence. In well-characterized micellar media, the (0,0) band of the $S_2 \leftarrow S_0$ absorption of pyrene is red-shifted by typically 2–3 nm relative to that in pure water.[16] For the AT polymers 2 and 3 the shift is 3 nm. I_1/I_3 in the pyrene fluorescence spectrum is a more sensitive indicator of medium polarity.[3] This ratio varies from 1.71 in water to 0.62 in cyclohexane.[3c] It takes a value of about 1.0–1.1 in anionic surfactant micelles,[4,5] ca. 1.2–1.5 in nonionic alkyl–ethylene oxide surfactant micelles,[4,6] and 1.3–1.6 in micelles formed from cationic surfactants.[4,7] We find that I_1/I_3 for pyrene equals 1.17 ± 0.01 in the aqueous associative thickener solutions when the polymer concentration is sufficiently high that almost all of the pyrene is partitioned into the hydrophobic domains. For polymer 2 this concentration is in excess of 1 wt %.

The I_1/I_3 ratio for bis(1-pyrenyl) methyl ether (referred to here as "dipyme") is also sensitive to the polarity of its environment.[11] This probe is insoluble in water but is solubilized in the presence of 2 or 3. For this probe in aqueous solutions of 2 and 3, we find I_1/I_3 = 1.30, which compares with the values found for dipyme in the following solvents: cyclohexane (0.65), cyclohexanol (1.12), dioxane (1.33), ethanol (1.35), 0.05 M SDS (1.40), acetone (1.49). The data from both probes indicate that the probes are partitioned into hydrophobic domains. These domains have a polarity somewhat more hydrophobic than that which they experience in an SDS micelle. We believe that this domain, the micelle-like cluster, must be sufficiently large to remove the probe from its aqueous surroundings.

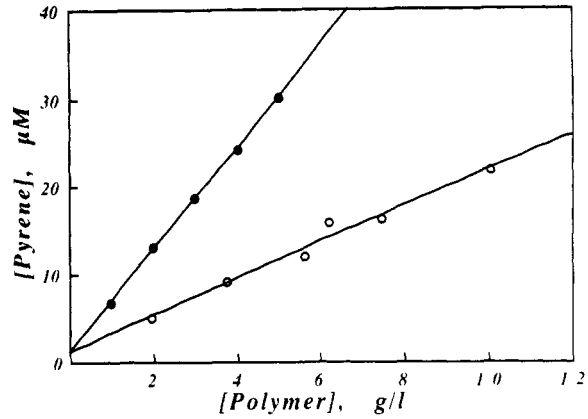

Figure 1. Total quantity of pyrene solubilized in aqueous solutions of associative thickeners. Measurements by UV spectrometry at room temperature. Top curve, polymer 2; bottom curve, polymer 3.

Partition Coefficients. Figure 1 shows the solubility behavior of pyrene in aqueous solutions of polymers 2 and 3 as determined by UV absorbance measurements. Notice that the maximum solubility[16,17] of pyrene in water, $[Py]_w^{sat}$, is 7×10^{-7} M. The data can be expressed as

$$[Py]_{total} = [Py]_w^{sat}(1 + 8.33[\text{polymer 2}]) \qquad (2)$$

$$[Py]_{total} = [Py]_w^{sat}(1 + 2.96[\text{polymer 3}]) \qquad (3)$$

where the polymer concentration is expressed in g/L. The slopes, when expressed in units of L of water/L of hydrophobe, would represent the desired partition coefficients K_v. Some of the salient features of these data are described below.

Within the limitation of the scatter of data points, a critical aggregation concentration (cac) is not discernible. We can set a limit to the cac being lower than 0.1 g/L, in agreement with an earlier report.[15] The major reason for the difference in the solubilizing ability of 2 and 3 is the difference in molecular weights; i.e., 2 has a greater number of cetyl groups per gram of polymer than 3. If the slopes of eqs 2 and 3 are expressed in molar units, we obtain 2.8×10^5 and 1.5×10^5 M^{-1}, respectively. This smaller relative difference may depend on less efficient cetyl end-labeling of 3 relative to 2 or some fundamental hydrophobe solubilizing ability of the two polymers. The variation of I_1/I_3 with the polymer concentration[15] can now be explained quantitatively in terms of the partitioning and emission of pyrene from water and hydrophobic phases. One can assume a pseudophase model of micelle formation. In this model we take the hydrophobic volume of $C_{16}H_{33}$-DI end labels proportional to the polymer concentration, assume a cluster density similar to liquid hexadecane (0.77 g/mL), and evaluate a hydrophobe molar volume of 1.1 L of cluster/mol of polymer. In this way, we calculate partition coefficients K_v of 2.2×10^5 and 1.2×10^5 (units: L of water/L of cluster) for 2 and 3, respectively.

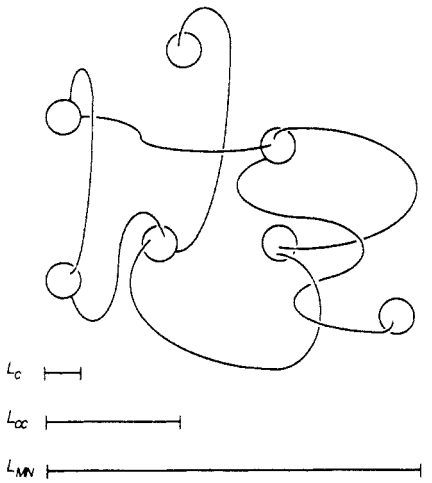

Figure 2. Schematic representation of a microgel network (MN). The circles represent micelle-like clusters (MLC's). For clarity, chains that cyclize to occupy the same cluster are not shown and only some possible chains interconnecting the MLC's are shown. The characteristic dimensions are defined in the text.

Almgren et al.[18] have reported on the solubility of pyrene in a series of micellar sodium alkyl sulfates (RSO_4Na). Applying the pseudophase model to their data, we calculate K_v as 1.2×10^5, 1.8×10^5, and 1.8×10^5 for R equal to C_{12}, C_{14}, and C_{16} linear alkyl chains, respectively.

In spite of differences in the systems considered, particularly the contribution of the isophorone diurethane (DI) group attached to the $C_{16}H_{33}O$ groups in the AT polymers, the magnitudes of K_v are remarkably similar. In a very different system,[16] the partitioning of pyrene in a series of polystyrene–poly(ethylene oxide) block copolymer micelles has K_v in the range (2–4) $\times 10^5$. Here the micellar aggregation numbers (50–300) and volumes vary considerably. The relative constancy of K_v expresses the relative constancy of the free energy for transfer of pyrene from an aqueous to a hydrocarbon environment. If the associative thickener MLC's had a one-digit aggregation number, pyrene molecules would spend a significant portion of their time neighboring other water molecules. We doubt that our partition coefficients would then be comparable to the class of larger micelles.

Microgel Network Model. A useful model for thinking about the properties of AT solutions in water is the microgel network (MN) model (cf. Figure 2).[34] In this model, a certain number of chain ends associate to form a micelle-like cluster. This cluster is characterized by a size (a diameter) L_c and a mean aggregation number, N_{agg}. Some of the chains cyclize so that both chain ends occupy the same cluster, whereas other chains span neighboring clusters. These chains provide the connectivity between micelles. In the MN model, a significant number of clusters can be connected. A second characteristic distance is the mean separation between clusters, L_{cc}. At modest polymer concentrations, e.g., 0.05–2 wt % for 2 or 3, we view the size of this network as finite. We think of it as a microgel whose characteristic dimension L_{MN} is likely to vary with the polymer concentration. At high enough concentration, the network spans the entire solution, which in turn forms a gel.

Remarkably, little is known with any degree of certainty about these polymer solutions. Among the parameters one would like to determine are the cluster size L_c and aggregation number N_{agg} (i.e., the number of $C_{16}H_{33}$ groups per cluster), the number of clusters per microgel N_{MN}, and the size of the microgel L_{MN}, all as a function of polymer concentration. Because fluorescence quenching experiments[12] in surfactant–micelle systems provide a convenient and reliable way of determining micelle mean aggregation numbers, we wished to apply these techniques here as a way of obtaining N_{agg} values.

Associative thickeners are used as rheology modifiers in aqueous solutions.[13,14,19] These solutions undergo strong shear thinning when subjected to a sufficiently strong shear force. While solutions of high molecular weight polymers are subject to shear thinning, they also store elastic energy. AT's are employed as spatter-suppressing rheology modifiers because they do not store elastic energy under shear. How this operates is not known, but in terms of the MN model, shear forces might have two quite different effects on the system. They may serve to break up the clusters. We can call this the MN-cluster fragmentation model. Or, through the concept of chain ends as "stickers",[20] the shear forces might only induce rapid hopping of chain ends among clusters. In this MN-cluster conservation model, rheological stresses are dissipated through rearrangement of the system, without affecting the total number of clusters present. That is, shear stresses reduce N_{MN} and L_{MN} but leave N_{agg} and L_c unchanged.

Understanding the mode of action of associative thickeners is going to require a detailed understanding of how the system responds to shear and other rheological stresses. Most rheological measurements on AT's are interpreted in terms of the MN-cluster fragmentation model. Recent fluorescence experiments by a group at Rohm and Haas,[21] employing pyrene-end-capped AT's, and further results from our laboratories[22] are more consistent with the MN-cluster conservation model for AT solutions subject to shear or extensional flow.

Quenching Kinetics. Rate Equations. In isotropic solution, fluorescence quenching normally follows Stern–Volmer kinetics[23]

$$\frac{I^0}{I} = \frac{\tau^0}{\tau} = 1 + k_q\tau^0[Q] \tag{4}$$

where I^0 and τ^0 refer to unquenched intensity and lifetime of the emission, respectively, [Q] is the bulk quencher concentration, and k_q is the second-order rate coefficient for the reaction. Depending upon efficiency of reaction upon encounter of the excited fluorophore with Q, the quenching reaction may or may not operate under diffusion control. In rigid matrices, fluorescence quenching commonly follows the Perrin static quenching model.[23]

$$\frac{I^0}{I} = \exp({}^4/_3\pi R_0{}^3[Q]) \tag{5}$$

In this model, quenching occurs instantaneously if Q is within a distance R_0 of the excited fluorophore and translational diffusion is not necessary.

Hydrophobic dyes in aqueous micellar systems normally exhibit Poisson quenching kinetics. Both the fluorophore and quencher aggregate into the micellar environment with a Poisson distribution. Under such circumstances the fluorophore decay rate $I(t)$ is given by[12a]

$$I(t) = I(0)\exp\left\{-\frac{t}{\tau^0} - \frac{[Q]}{[mic]}(1 - e^{-kt})\right\} \tag{6}$$

In this expression, [mic] refers to the molar concentration of micelles in the solution. The t/τ^0 term describes the exponential decay of fluorophore in micelles containing no quencher. The second term describes the contribution to the total observable fluorescence intensity from micelles

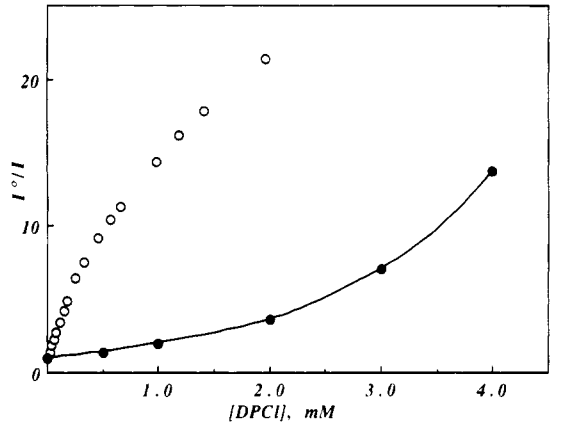

Figure 3. Stern–Volmer plots of the fluorescence of 6×10^{-7} M pyrene quenched by dodecylpyridinium chloride (DPCl). Left curve, aqueous 5.0 g/L solution of **2**; right curve, aqueous 0.05 M solution of SDS.

containing i quenchers (i = 1, 2, 3, ...), and k is the corresponding pseudo-first-order rate coefficient for the intramicellar reaction with one quencher. When k is very large, so that intramolecular quenching is very efficient, integration of eq 6 yields (7), the classic static quenching model used to analyze micellar quenching by steady-state fluorescence measurements.[24]

$$\ln \frac{I^0}{I} = \frac{[Q]}{[mic]} = \frac{[Q]N_{agg}}{[surfactant] - cmc} \qquad (7)$$

Data analysis in terms of eq 7 is justified only when the intramicellar quenching reaction is fast and efficient.

Quenching by Pyridinium Salts. One of the well-studied quenchers[25] of pyrene fluorescence is the surfactant dodecylpyridinium chloride (DPCl). Figure 3 shows the comparison of such quenching experiments in a 5.0 g/L solution of **2** and a 0.05 M solution of SDS. The pyrene concentration is sufficiently dilute that excimer formation is negligible. Surfactant SDS follows a nearly exponential form represented by eq 7, yielding an aggregation number of 59. Polymer **2** shows an unusual behavior. Up to 0.2 mM DPCl, where about 80% of the intensity is quenched, the data fit a nearly perfect straight line (slope $\approx 2.2 \times 10^4$ M^{-1}). Above 0.2 mM DPCl, the plot deviates from linearity with a negative curvature, a case usually ascribed to protected quenching.[26] Since DPCl is itself a surfactant, at its higher concentrations it may also perturb the polymer association.[14,27] However, even when the DPCl concentration is less than 2 orders of magnitude below its cmc (≈0.01 M), the observed quenching behavior is Stern–Volmer-like and does not follow eq 7. Given a lifetime of pyrene monomer τ_M^0 of 240 ns in our system, we calculate an apparent quenching constant $k_q \approx 1 \times 10^{11}$ M^{-1} s^{-1}, an order of magnitude faster than possible for diffusion-controlled reactions in water. Something unusual is occurring in this system.

Pyrene Excimer Formation. At elevated pyrene concentration in solutions of associative thickeners, excimer emission is observed. Excimer formation is a well-known phenomenon[29] resulting in the self-quenching of excited monomer fluorescence I_M and the rise of a new excited dimer (excimer) emission I_E. Excimer kinetics have been studied in surfactant micellar systems and used for the evaluation of aggregation numbers.[29] In a typical steady-state experiment, one varies [Py] at a fixed [micelle] and measures I_E and I_M, evaluating I_E/I_M. The latter is equal to the relative excimer to monomer luminescence yields Y_E/Y_M. Figure 4 shows typical spectra

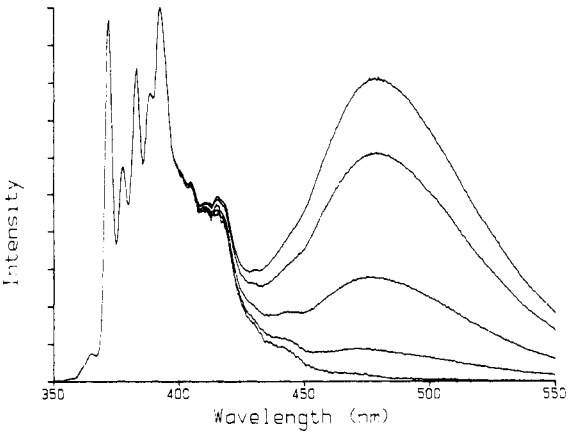

Figure 4. Fluorescence spectra of pyrene solubilized in 10 g/L aqueous solutions of **2**. From top to bottom, [Py] = 60, 45, 20, 6, and 0.2 μM. Excitation wavelength at 338 nm, spectral bandpass 1 nm.

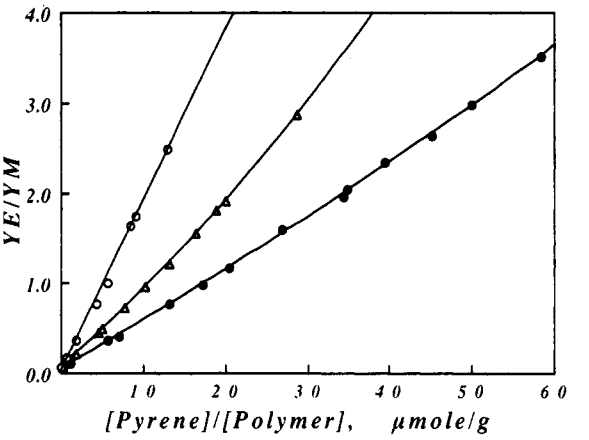

Figure 5. Relative excimer to monomer fluorescence yields of pyrene in aqueous solutions of polymer **2**. From top to bottom, [2] = 2.3, 5.0, and 10.0 g/L, respectively. The horizontal axis represents the micellized pyrene concentration.[22]

obtained when the associative thickener **2** solution is fixed at 10 g/L while the pyrene concentration is varied. The blue monomer fluorescence shows vibrational fine structure with the I_1/I_3 ratio sensitive to the local medium polarity as described above. The intensity of the broad green excimer fluorescence is sensitive to [Py]. Similar data are obtained with [2] equal to 5.0 and 2.3 g/L. The spectra show two general features. The excitation spectra of the excimer (520 nm) and monomer (392 nm) are identical, showing a lack of ground-state preassociation.[30] I_1/I_3 is very much a constant (±0.01) independent of [Py]. In our most concentrated pyrene solution about 50% of excited monomers are self-quenched. If pyrene emission were occurring from regions of significantly different micropolarity and microscopic viscosity, we would have noticed a change in I_1/I_3. The ratio is 1.17, 1.19, and 1.21 for [2] being 10, 5.0, and 2.3 g/L, respectively. The slight change in the ratio occurs because more pyrene is partitioned into the water phase as [2] decreases.[15] Figure 5 shows the dependence of Y_E/Y_M on the micellized pyrene concentration[31] for three different concentrations of polymer **2**.

Before we discuss our results, it would be pertinent to review some of the general features of such experiments in the simpler surfactant micelle systems. The behavior usually observed in these systems is that as [Py] is increased for fixed [micelle] so too is Y_E/Y_M. This is simply a result of the fact that at higher [Py], the encounter probability of two pyrene molecules increases. In non-

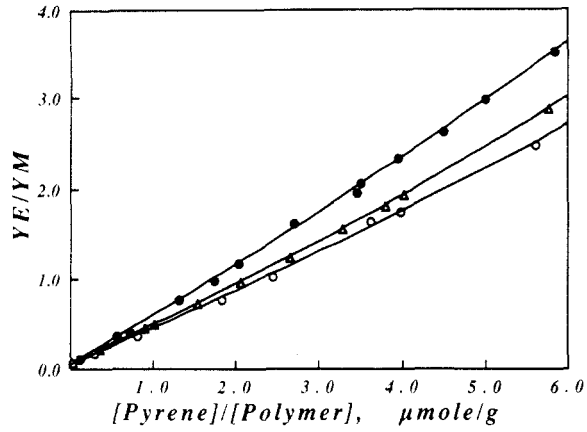

Figure 6. Data of Figure 5 plotted as a function of local concentration of pyrene, i.e., [pyrene]/[polymer]. From top to bottom, [2] = 10.0, 5.0, and 2.3 g/L.

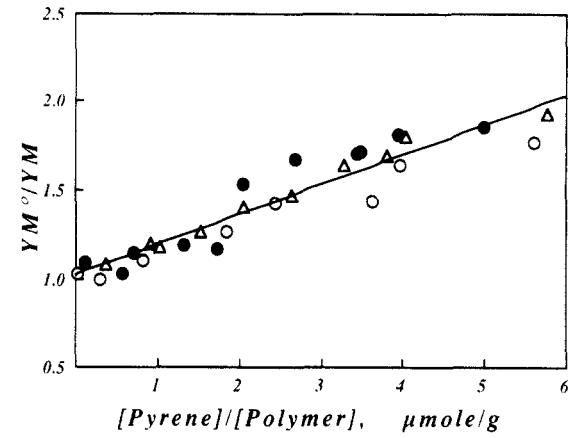

Figure 7. Stern–Volmer plots of the self-quenching of pyrene monomer fluorescence. Data from analysis of steady-state experiments described in the text. (●) [2] = 10 g/L; (△) [2] = 5.0 g/L; (○) [2] = 2.3 g/L.

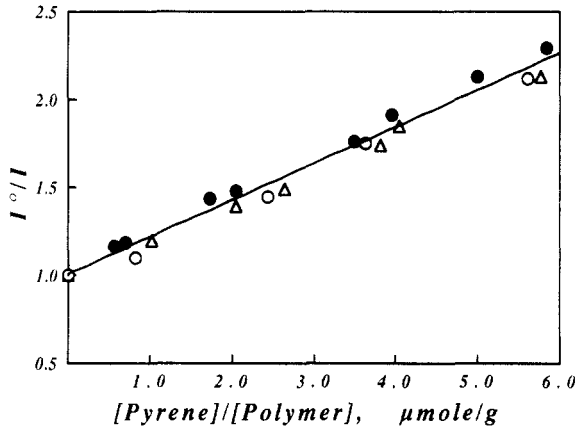

Figure 8. Stern–Volmer plots of the self-quenching of pyrene monomer fluorescence. Data from analysis of fluorescence decay measurements described in the text. (●) [2] = 10 g/L; (△) [2] = 5.0 g/L; (○) [2] = 2.3 g/L.

micellar homogeneous fluid media,[28] Y_E/Y_M is linearly dependent on [Py], while in micellar media, a positive curvature is observed.[29] At any fixed [Py], a decrease in [micelle] results in an increase of Y_E/Y_M. The latter occurs because a decrease of [micelle] implies a decrease of the available hydrophobic volume and a concurrent increase of the effective average local pyrene concentration. Figure 5 shows that pyrene in solutions of polymer **2** also display the general features discussed above.

A distinguishing characteristic of many surfactant micelle systems is their simplicitly. By this we mean that in these systems micelles are almost monodisperse in size. As a case in point, the surfactant SDS forms spherical micelles with an aggregation number of about 60, and this property is retained as the surfactant concentration is increased by 1 order of magnitude over its cmc.[32] The uniformity of size and aggregation number, in turn, implies Y_E/Y_M should be a universal function of the mean number of pyrene molecules per micelle, [Py]/[micelle]. That is, if [micelle] were changed, Y_E/Y_M would remain a constant, as long as [Py]/[micelle] is a constant. Figure 6 shows a plot of the Y_E/Y_M data vs [Py]/[polymer]. We note that in our system the cac is less than 0.1 g/L, so that [polymer] is equal to N_{agg}[micelle]. Clearly, in the associative thickener solutions, Y_E/Y_M is not a universal function of [Py]/[polymer]. For a fixed pyrene to polymer ratio, the data reveal that a higher [polymer] affords an environment more favorable to excimer formation. The deviation from universality is small but distinct.

There are several ways of explaining the observed effect. An intermicellar mode of excimer formation could explain both the near-linear plots of I_E/I_M vs [Py] and the enhanced excimer formation efficiency at higher [polymer]. Since pyrene can diffuse in water no more than 60–100 Å in its unquenched monomer lifetime ($\tau_M^0 \approx 240$ ns in the micelle, $\tau_M^0 \approx 140$ ns in air-saturated water), intermicellar hopping would require that the spacing between clusters (L_{cc} in Figure 2) be much shorter than that anticipated from the star-model theory of nonionic micelles.[33]

Alternatively, it might be that N_{agg} grows as [polymer] is increased, but this is not supported by the self-quenching data given below. The most plausible explanation is that increasing [polymer] affords more protection against oxygen quenching of the fluorescent states, effectively increasing the luminescence quantum yields. Our decay measurements show a monomer lifetime of 230–240 ns. The excimer lifetime is shorter, about 50 ns, and more difficult to determine as accurately.

Monomer Fluorescence Self-Quenching. The relative monomer fluorescence yields have been extracted from our steady-state and dynamic luminescence measurements by the procedures described in the experimental section. Figure 7 shows a Stern–Volmer type plot of Y_M^0/Y_M vs [Py]/[polymer] for the three sets of [2]. Y_M^0 is the pyrene monomer fluorescence yield in the limit of infinite dilution (in pyrene). The three sets of data seem to follow a universal correlation, but due to effects explained in the Experimental Section, the scatter of data points is large. Figure 8 shows the same plot for data evaluated from luminescence decay measurements. We notice that Y_M^0/Y_M is a universal function of [Py]/[polymer] and that there is good agreement between the data sets of Figures 7 and 8. The positive curvature, if any, is small, and Y_M^0/Y_M follows a near-linear dependence on [Py].

In summary, pyrene monomer self-quenching and pyrene quenching by DPCl exhibit a kinetic behavior much more in accord with an apparent Stern–Volmer diffusional quenching model than with the usually observed Poisson quenching expected for micellar systems. To explain these results, further information about the micellar environment is needed.

Excimer Formation in Dipyme. Dipyme is a particularly interesting probe for microheterogeneous systems because it conveys two independent types of information about its environment. In the monomer emission band, I_1/I_3 is a sensitive probe of medium polarity.[11] This feature of the emission was discussed above in establishing that dipyme is solubilized by AT solutions into hydrophobic domains. In addition, the extent of excimer formation

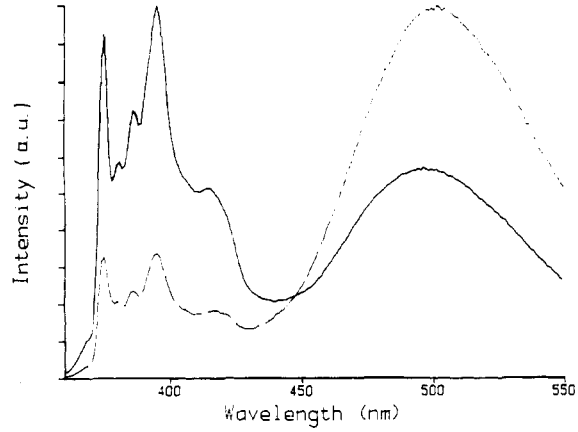

Figure 9. Fluorescence spectra of 1×10^{-6} M dipyme molecularly solubilized in aqueous solutions of 5.0 g/L 2 (solid trace) and 0.05 M SDS (dashed trace). Excitation wavelength at 346 nm, spectral band-pass 2 nm.

(e.g., I_E/I_M) is very sensitive to the local friction ("microviscosity") which resists the conformational changes necessary to bring the two pyrene groups together.

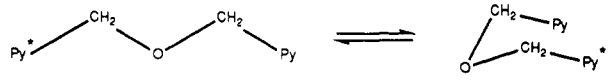

In Figure 9 we display together fluorescence spectra of dipyme dissolved in aqueous SDS micelles and also solubilized by a 0.5 wt % solution of **2**. One notes immediately that the excimer intensity is much lower in the AT polymer solution, indicating a much more viscous environment than in the SDS micelles. By comparison with other experiments, the microviscosity of the AT clusters is much closer to that of phospholipid bilayers[11a] than that of typical surfactant micelles.[10] We note that I_E/I_M values for dipyme in solutions of **2** and **3** are very similar and do not vary with changes in polymer concentration.

Poisson Quenching in Rigid Micelles. In rigid micelles, diffusive mobility is expected to be very slow. To get effective quenching, one may have to add sufficient quencher to obtain multiple occupancy of each micelle by quencher molecules. For example, if N_{agg} for the MLC's is on the order of 30, 50% self-quenching in Figure 8 corresponds to 2.5 pyrenes per micelle. If $N_{agg} = 60$, then there are 5 pyrenes per micelle. When the mean occupancy is large, the Poisson distribution narrows, and it becomes meaningful to talk about the mean local concentration. Furthermore, the local rigidity implies slow rates of intramicellar self-quenching for pyrene; i.e., k of eq 6 is smaller than $1/\tau^0$. The latter means that for the greater portion of decay, $e^{-kt} \approx 1 - kt$, and in this way integration of eq 6 yields a Stern–Volmer type of relationship.

$$\frac{I^0}{I} \approx 1 + \frac{k\tau^0}{[\text{mic}]}[Q] = 1 + k_q\tau^0[Q_m] \qquad (8)$$

Here, k_q is k times the micellar molar volume and $[Q_m]$ is the mean local concentration of quenchers in the available hydrophobic volume (moles of Q/volume of micelles). Equation 8 rationalizes apparent Stern–Volmer behavior without doing away with Poisson kinetics. From the molecular weight of **2**, assuming two $C_{13}H_{33}O$-DI end groups per chain and assuming a hydrocarbon droplet-like density for the clusters, we can calculate a micellar volume of 1.1 L/mol of micelle. The slope of Figure 8 equals 0.21 g of polymer/μmol of pyrene. This equates $k_q\tau^0$ with 7.2 L of hydrophobe/mol of pyrene, yielding a diffusion-controlled local quenching constant $k_q \approx 3 \times 10^7$ M^{-1} s^{-1}. Similarly, for the DPCl quenching experiments we calculate $k_q \approx 2 \times 10^7$ M^{-1} s^{-1}. These values are satisfying because they correspond to diffusion-controlled quenching rates in media some 2 orders of magnitude more viscous than water and are in accord with observations of the luminescence behavior of dipyme in the aqueous associative thickener solutions.

Conclusions

$C_{16}H_{33}O$-end-capped poly(ethylene oxide) associative thickener polymers self-associate in water. The self-association process involves end-group aggregation to form hydrophobic micelle-like clusters. These MLC's are sufficiently large that organic dye molecules containing one or two pyrene groups can be solubilized and within the cluster experience a hydrophobic environment comparable to that of an SDS micelle. Unlike SDS micelles,[10a] the MLC's are more rigid and less fluid. While fluorescence quenching experiments with hydrophobic dyes appear to be very effective, the quenching follows a rate law seemingly inconsistent with the classic Poisson model that typifies quenching in micellar systems. A careful analysis of the quenching kinetics reveals that quenching is in fact rather inefficient in terms of the relatively large amount of quencher per micelle required. This is a direct consequence of the low microfluidity of the hydrocarbon phase in the clusters.

With an insensitive Poisson quenching effect, we are still unable to determine mean aggregation numbers from our quenching data. Previous experiments by Richey et al. have inferred small aggregation numbers through pyrene excimer experiments[21] in which the data analysis invoked assumptions of fast and efficient quenching in the clusters. Because this assumption is incorrect, it is likely that the true aggregation number of their system is significantly larger.

Acknowledgment. The authors would like to thank the Ontario Centre for Materials Research, NSERC Canada, Union Carbide, and Aqualon for their generous support of this research.

References and Notes

(1) Current address: Thomson TRT Defense, Rue Guynemer, 78283 Guyancourt, France.
(2) (a) Zana, R. In *Surfactant Solutions: New Methods of Investigation*; Zana, R., Ed.; Marcel Dekker: New York, 1986. (b) von Bünau, G.; Wolff, T. In *Advances in Photochemistry*; Volman, D. H., Hammond, G. S., Gollnick, E., Eds.; John Wiley & Sons: New York, 1988. (c) Chu, D. Y.; Thomas, J. K. In *Photochemistry and Photophysics*; Rabek, J. F., Ed.; CRC Press: Boca Raton, FL, 1991; Vol. 3, pp 49–102.
(3) (a) Nakajima, A. *J. Lumin.* **1976**, *11*, 429. (b) Glushko, V.; Thaler, M. S. K.; Karp, C. D. *Arch. Biochem. Biophys.* **1981**, *210*, 33. (c) Dong, D. C.; Winnik, M. A. *Can. J. Chem.* **1984**, *62*, 2560.
(4) (a) Kalyanasundaram, K.; Thomas, J. K. *J. Am. Chem. Soc.* **1977**, *99*, 2039. (b) Kalyanasundaram, K. *Langmuir* **1988**, *4*, 842.
(5) (a) Ohiashiki, T.; Mohri, T. *Chem. Pharm. Bull.* **1978**, *26*, 3161. (b) Lianos, P.; Zana, R. *J. Phys. Chem.* **1980**, *84*, 3339.
(6) (a) Turro, N. J.; Kuo, P.-L. *Langmuir* **1986**, *2*, 438. (b) Turro, N. J.; Kuo, P.-L. *J. Phys. Chem.* **1986**, *90*, 837.
(7) (a) Lianos, P.; Lang, J.; Zana, R. *J. Colloid Interface Sci.* **1983**, *91*, 276. (b) Malliaris, A.; Paleos, C. M. *Ibid.* **1984**, *101*, 364.
(8) (a) Kalyanasundaram, K.; Thomas, J. K. *J. Phys. Chem.* **1977**, *81*, 2176. (b) Turro, N. J.; Kuo, P.-L. *Langmuir* **1985**, *1*, 170. (c) Ueda, E.; Schelly, Z. A. *Langmuir* **1989**, *5*, 1005. (d) Buncel, E.; Rajagopal, S. *Acc. Chem. Res.* **1990**, *23*, 226.
(9) (a) Shinitzky, M.; Dianoux, A. C.; Gitler, C.; Weber, G. *Biochemistry* **1973**, *10*, 2106. (b) Keh, E.; Valeur, B. *J. Colloid Interface Sci.* **1981**, *79*, 465. (c) Reference 3d. (d) Jobe, D. J.; Verrall, R. E. *Langmuir* **1990**, *6*, 1750.

(10) (a) Turro, N. J.; Aikawa, M.; Yekta, A. *J. Am. Chem. Soc.* **1979**, *101*, 772. (b) Zachariasse, K. A. In *Excited State Probes in Biochemistry and Biology*; Szabo, A., Ed.; Plenum: New York, 1985. (c) Kano, K.; Ueno, Y.; Hashimoto, S. *J. Phys. Chem.* **1985**, *89*, 3161.
(11) (a) Georgesauld, D.; Desmaséz, R.; Lapouyade, R.; Babeau, A.; Richard, H.; Winnik, M. A. *Photochem. Photobiol.* **1980**, *31*, 539. (b) Winnik, F. M.; Winnik, M. A.; Ringsdorf, H.; Venzmer, J. *J. Phys. Chem.* **1991**, *95*, 2583.
(12) (a) Yekta, A.; Aikawa, M.; Turro, N. J. *Chem. Phys. Lett.* **1979**, *63*, 543. (b) Warr, G. G.; Grieser, F. *J. Chem. Soc., Faraday Trans.* **1986**, *82*, 1813. (c) Thomas, J. K. *J. Phys. Chem.* **1987**, *91*, 267. (d) Tachiya, M. In *Kinetics of Nonhomogeneous Processes*; Freeman, G. R., Ed.; John Wiley & Sons: New York, 1987; pp 575–650.
(13) (a) Fikentscher, R.; Oppenländer, K.; Müller, R. Ger. Pat. 2 054 885, 1972. (b) Singer, W.; Tenneck, N. J.; Doiscoll, A. E. U.S. Pat. 3 770 684, 1973. (c) Emmons, W. D.; Stevens, T. E. U.S. Pat. 4 079 028, 1978. (d) Glass, J. E.; Fernando, R. H.; Egland-Jongewaard, S. K.; Brown, R. G. *JOCCA* **1984**, *10*, 256. (e) Schaller, E. J.; Sperry, P. R. In *Handbook of Coatings Additives*; Calbo, L. J., Ed.; Marcel Dekker: New York, 1992; Vol. II, Chapter 4. (f) Howard, P. R.; Leasure, E. L.; Rosier, S. T.; Schaller, E. J. *J. Coat. Technol.* **1992**, *64*, 87.
(14) Jenkins, R. D. Ph.D. Thesis, Lehigh University, Bethlehem, PA, 1990.
(15) Wang, Y.; Winnik, M. A. *Langmuir* **1990**, *6*, 1437.
(16) Wilhelm, M.; Zhao, C.-L.; Wang, Y.; Xu, R.; Winnik, M. A. *Macromolecules* **1991**, *24*, 1033.
(17) Schwartz, F. P. *J. Chem. Eng. Data* **1977**, *22*, 273.
(18) Almgren, M.; Grieser, F.; Thomas, J. K. *J. Am. Chem. Soc.* **1979**, *101*, 279.
(19) (a) Bielmann, J. H.; Riesthuis, F. J. J.; van der Velden, P. M. *J. Polym. Paints Colours* **1986**, *176*, 450. (b) Glass, J. E. *Water Soluble Polymers*; ACS Adv. Chem. Ser. 213; American Chemical Society: Washington, DC, 1986. (c) Glass, J. E. *Polymers in Aqueous Media*; ACS Adv. Chem. Ser. 223; American Chemical Society: Washington, DC, 1989. (d) Glass, J. E.; Karunasena, A. *Polym. Mater. Sci. Eng.* **1989**, *61*, 145. (e) Jenkins, R. D.; Silebi, C. A.; El-Aasser, M. S. *Polym. Mater. Sci. Eng.* **1989**, *61*, 629. (f) Jenkins, R. D.; Silebi, C. A.; El-Aasser, M. S. In *Advances in Emulsion Polymerization and Latex Technology: 21st Annual Short Course*; El-Aasser, M. S., Ed.; Lehigh University, June 1990, Chapter 17. (g) Balazs, A. C.; Hu, J. Y.; Lentvorski, A. P. *Phys. Rev. A* **1990**, *41*, 2109. (h) Schultz, D. N.; Glass, J. E. *Polymers as Rheology Modifiers*; ACS Symp. Ser. 462; American Chemical Society: Washington, DC, 1991. (i) Maechling-Strasser, C.; Françoise, J.; Clouet, F.; Tripette, C. *Polymer* **1992**, *33*, 627. (j) Persson, K.; Abrahmsén, S.; Stilbs, P.; Hansen, F. K.; Walderhaug, H. *Colloid Polym. Sci.* **1992**, *270*, 465.
(20) Witten, T. A. *J. Phys. (Les Ulis Fr.)* **1988**, *49*, 1055.
(21) Richey, B.; Kirk, A. B.; Eisenhart, E. K.; Fitzwater, S.; Hook, J. *J. Coat. Technol.* **1991**, *63* (798), 31.
(22) Vlahiotis, D. Ph.D. Thesis, University of Toronto, Toronto, Canada, 1992.
(23) Lakowicz, J. R. *Principles of Fluorescence Spectroscopy*; Plenum: New York, 1983.
(24) Turro, N. J.; Yekta, A. *J. Am. Chem. Soc.* **1978**, *100*, 5951.
(25) (a) Hashimoto, S.; Thomas, J. K. *J. Colloid Interface Sci.* **1984**, *106*, 152. (b) Chu, D.; Thomas, J. K. *J. Am. Chem. Soc.* **1986**, *108*, 6270. (c) Malliaris, A.; Lang, J.; Zana, R. *J. Phys. Chem.* **1986**, *90*, 655. (d) Muto, Y.; Esumi, K.; Meguro, K.; Zana, R. *J. Colloid Interface Sci.* **1987**, *120*, 162. (e) Reekmans, S.; Luo, H.; Van der Auweraer, M.; De Schryver, F. C. *Langmuir* **1990**, *6*, 628. (f) Binana-Limbele, W.; van Os, N. M.; Rupert, L. A. M.; Zana, R. *J. Colloid Interface Sci.* **1991**, *141*, 157.
(26) (a) Lakowicz, J. R. *Principles of Fluorescence Spectroscopy*; Plenum: New York, 1983; p 280. (b) Winnik, M. A.; Disanayaka, B.; Pekcan, O.; Croucher, M. *J. Colloid Interface Sci.* **1990**, *139*, 251. (c) Yekta, A.; Duhamel, J.; Winnik, M. A. *J. Chem. Phys.* **1992**, *97*, 1154.
(27) (a) Thibeault, J. C.; Sperry, P. R.; Schaller, E. J. In *Water Soluble Polymers*; Glass, J. E., Ed.; Adv. Chem. Ser. 213; American Chemical Society: Washington, DC, 1986; Chapter 20. (b) Bassett, D. R.; Glancy, C. W. Division of Colloid and Surface Chemistry, Paper 31, American Chemical Society National Meeting, Miami Beach, 1989. (c) Balazs, A. C.; Hu, J. Y. *Langmuir* **1989**, *5*, 1230. (d) Balazs, A. C.; Hu, J. Y. *Langmuir* **1989**, *5*, 1253.
(28) Birks, J. B. *Photophysics of Aromatic Molecules*; Wiley-Interscience: New York, 1970.
(29) (a) Selinger, B. K.; Watkins, A. R. *Chem. Phys. Lett.* **1978**, *56*, 99. (b) Infelta, P. P.; Grätzel, M. *J. Chem. Phys.* **1979**, *70*, 179. (c) Atik, S. S.; Nam, M.; Singer, L. A. *Chem. Phys. Lett.* **1979**, *67*, 75.
(30) Reynders, P.; Kühnle, W.; Zachariasse, K. *J. Am. Chem. Soc.* **1990**, *112*, 3929.
(31) Of the total amount of pyrene solubilized, a small fraction (1–5%) is always partitioned into the water phase. The quantity of micellized pyrene can be calculated from the partitioning data as $[Py]_{micelle} = 8.33\,[Py]_{total}\,[2]/(1 + 8.33[2])$, where [2] is expressed in g/L units.
(32) Croonen, Y.; Geladé, E.; Van der Zegel, M.; Van der Auweraer, M.; Vandendriessche, H.; De Schryver, F. C.; Almgren, M. *J. Phys. Chem.* **1983**, *87*, 1426.
(33) Halperin, A. *Macromolecules* **1987**, *20*, 2943.
(34) A referee has reminded us of how sensitive some scientists are to the choice of nomenclature pertaining to micelles and other associated structures. For complex systems of the sort examined here, a proper choice of words to describe the system requries a much deeper understanding of the structure of the system than we have at present. Thus the choice of words one uses may evolve as our knowledge grows. Here we try to develop a descriptive language in terms of the microgel network model. As we come to appreciate new features of the system and modify the model accordingly, some of the terms we use may also have to be modified.